

# Flow properties of PLZTN aqueous suspensions for tape casting

Davide Gardini, Marco Deluca<sup>1</sup>, Marco Nagliati<sup>2</sup>, Carmen Galassi<sup>\*</sup>

*National Research Council (CNR), Institute of Science and Technology for Ceramics (ISTEC), Via Granarolo 64, I-48018 Faenza, Italy*

Received 4 January 2010; received in revised form 16 January 2010; accepted 2 March 2010

Available online 24 April 2010

## Abstract

Several aqueous suspensions of lead zirconate titanate powder doped with lanthanum and niobium (PLZTN) were prepared, tape cast and characterized by rheological measurements in steady shear flow. Experimental data were fitted by some viscous models available on literature and the model parameters compared in order to obtain information about the effects of the composition on suspension viscosity. Such approach represents a necessary step in the desirable optimization of tape casting process, which includes also the analysis by flow simulations. Five viscous models have been considered: from the classic plastic models of Bingham and Herschel–Bulkley, to the modified plastic model of Papanastasiou, up to the pseudoplastic models of Cross and Roberts–Barnes–Carew. The parameter-based comparison was carried on with the latter, resulting, with its eight parameters, the best-fit model, while for flow simulation purposes the ones with few parameters, as the Cross and Herschel–Bulkley models, resulted the more appropriate from some simple considerations.

© 2010 Elsevier Ltd and Techna Group S.r.l. All rights reserved.

**Keywords:** A. Tape casting; Viscosity; Aqueous suspension; PLZTN

## 1. Introduction

In the past 20 years, tape casting has gathered importance in the ceramic industry as a process suitable to obtain thin ceramic layers, necessary for the production of multilayer textures employed in structural applications, electrodes for solid oxide fuel cells (SOFC) and electronic devices [1–3]. In particular, suspensions of perovskitic powders are tape cast in order to obtain multilayer ferroelectric structures to be used as capacitors or sensor/actuator devices. For piezoelectric applications, lead zirconate titanate (PZT)-based materials are still the most important.

In the tape casting process, a well-dispersed suspension of ceramic particles in an organic medium or in water is poured into a tape casting head constituted by a reservoir and a doctor blade, whose height is adjustable with micrometric screws [4]. The slurry is then shaped in a thin layer onto a polymeric carrier

film as a consequence of the motion either of the head or of the carrier film itself. The ceramic tape so obtained is dried and removed from support, and subsequently subjected to thermal–mechanical treatments (depending on applications) like cutting, electrode screen-printing, piling, lamination, debonding and sintering.

In the optimization of the tape casting process, from the pouring of the suspension in the reservoir to the handling of as-cast tapes, as well as to the quality of the tapes, a key role is played by the additives added to the suspension as dispersants, binders, plasticizers and surfactants. Usually, all additives contribute, in some extent, to determine the quality of the tapes, directly or indirectly through their influence on the suspension rheology from which the filling of the reservoir, the flow under the doctor blade and the leveling of the tapes depend. In particular, the handling capability of the dried tape, which is one of the main requirements to have a good tape, together with the absence of flaws, is mainly controlled by the binder and plasticizer. This point is further stressed if an aqueous medium is used as dispersing liquid, in the light of the “green processing” aimed at avoiding environmental and safety problems. If compared to the well-known organic suspensions for tape casting, the research on the water-based ones demands for extended developments. At present, significant drawbacks affect the performances of aqueous suspensions for tape casting, mainly concerning the

<sup>\*</sup> Corresponding author. Tel.: +39 0546 699750; fax: +39 0546 46381.

E-mail address: [carmen.galassi@istec.cnr.it](mailto:carmen.galassi@istec.cnr.it) (C. Galassi).

<sup>1</sup> Current addresses: (1) Materials Center Leoben Forschung GmbH, Roseggerstr. 12, A-8700 Leoben, Austria; (2) Montanuniversität Leoben, Institut für Struktur- und Funktionskeramik, Peter-Tunner-Str. 5, A-8700 Leoben, Austria.

<sup>2</sup> Current address: Brembo SGL Carbon Ceramic Brakes, Viale Europa 2, I-24040 Stezzano, BG, Italy.

nature and the extent of the interactions between the charged surfaces of the powders and the polar medium. This requires to carefully control the rheology of the aqueous slurries by proper balances of additives and to study their interactions with powders and dispersing medium.

For successful applications, the slurries for tape casting should show a shear-thinning behavior with a low enough viscosity at the shear rates typical of the casting process (to ensure appropriate flow conditions under the blade) and higher viscosity at the low-shear stresses generated immediately after the blade. Moreover, in this second step, the viscosity should undergo a fast increase to prevent undesired flow and sedimentation of the ceramic particles; thixotropy or other time-dependent behavior is not desired [5].

When the contribution of additives to suspension viscosity is negligible, their concentrations are adjusted through a trial-and-error procedure directly based on the casting performance. In the other cases, an analysis of the rheological behavior based on a systematic experimental characterization can provide a rational basis, not only to determine whether a suspension exhibits the desired flow properties, but also to perform useful comparisons between different systems to investigate the role played by additives. This approach requires the choice of rheological models suitable to correlate the experimental data with satisfactory approximation, namely able to fit the dependence of viscosity on shear rate (or shear stress) over extended experimental ranges. Several rheological equations are available in literature to describe the plastic behavior of concentrated suspensions and other complex fluids, as, e.g., the Bingham and Herschel–Bulkley models where a yield stress sharply marks the onset of flow conditions. After the introduction on the market of sophisticated controlled-stress rheometers, the experimental window has been considerably expanded towards lower shear rates and stresses, so as to find the lower Newtonian plateau and the zero-shear viscosity even in the case of concentrated dispersions. Consequently, the concept of yield stress has been redefined and addressed as an “engineering reality” [6]. In order to describe the flow behavior from low- to high-shear rates, more complex equations must be considered as, e.g., a modification of the Bingham equation [7] where a gradual stress growth before yielding is added (Papanastasiou [8]), or models able to predict both the Newtonian plateaus like those proposed by Cross [7] and Carreau [9]. However, also the latter equations can result inadequate to describe the stress dependence of viscosity, especially when a marked viscosity drop is observed in a narrow stress range. In such cases a satisfactory data correlation from the lower Newtonian region to the upper one, also when the profile of the flow curve is asymmetric, is generally provided by the Roberts–Barnes–Carew model, an extended version of the Ellis model, owing to its eight adjustable parameters [10]. On the contrary, in the case of systems where the viscosity drop is not well pronounced the latter model may encounter some difficulties in obtaining precise values of the critical stress. Souza Mendes and Dutra [9] have proposed a four-parameter equation and a method based on the minimum derivative of shear stress and shear rate logarithms which is effective to recognize the transition from solid-like to liquid-like behavior.

The quality of fitting is obviously related to the number of adjustable parameters and can be improved by using more flexible equations, but as rule of thumb one should use models with as few parameters as possible, compatibly with a satisfactory correlation with the experimental data. This works especially for the application to flow simulation problems where models with few parameters permit to solve more easily the numerical iterations and to reduce the calculation time.

Studies on the effects of additives compared via model parameters have been performed in several works on aqueous ceramic suspensions for tape casting, applying the Herschel–Bulkley equation on PZT suspensions (Feng and Dogan [17]) and on alumina suspensions (Pagnoux et al. [18]), and the Casson model on zirconia suspensions (Bitterlich et al. [5]).

The aim of the present work is to study the effect of additives on the flow properties of aqueous PZT suspensions for tape casting, through a parameter-based comparison between different formulations. Data fitting has been performed with a set of models ranging from plastic (Bingham, Herschel–Bulkley, Papanastasiou) to shear-thinning (Cross, Roberts–Barnes–Carew) type. The last model has been recognized as the most suitable for representing the flow behavior of the considered suspensions, and, hence, the aforementioned comparison was referred to its parameters. The observation of the casting performances of the slurries showed that other factors are involved in the optimization of the tape casting process. Anyway, a rheological characterization of suspensions is the first step toward the process optimization. Finally, in view of next flow simulations of tape casting process to solve technological problems, the applicability of the above viscous models to the numerical treatment has been qualitatively discussed.

## 2. Experimental procedure

### 2.1. PLZTN powders

Powders of composition  $(\text{Pb}_{0.93}\text{La}_{0.07})[(\text{Zr}_{0.60}\text{Ti}_{0.40})_{0.9825}\text{Nb}_{0.0175}]\text{O}_3$  (PLZTN) were synthesized by solid state reaction of the starting oxides (Table 1). The powder synthesis process was the following: (i) ball milling in plastic jars for 48 h (with  $\text{ZrO}_2$  spheres as milling media) of the stoichiometric amounts of oxides dispersed in water, except for lead oxide that is added with an excess of 3.26 wt% to compensate lead volatilization during sintering; (ii) freeze drying of suspension; (iii) sieving at 250  $\mu\text{m}$ ; (iv) heat treatment in air at 850 °C for 4 h in a zirconia crucibles; (v) wet ball milling in ethanol for 100 h using plastic jars with  $\text{ZrO}_2$  spheres as milling media; (vi) drying in oven at 90 °C; (vii) sieving at 250  $\mu\text{m}$ . Some properties of the synthesized PLZTN powders are reported in Table 2.

### 2.2. Suspensions preparation

PLZTN powder suspensions were electrosterically stabilized by addition of ammonium polyacrylate with low molecular weight (2500 g/mol) available as 40 wt% aqueous solution (Duramax D-3021, Rohm & Haas, Philadelphia, USA). This polyelectrolyte provides an electrostatic barrier to

Table 1  
Characteristics of the starting oxides.

Oxide	Producer	Purity [%]	S.S.A. [m <sup>2</sup> /g]	Grain size <sup>a</sup> [μm]	<i>d</i> <sub>50</sub> <sup>b</sup> [μm]	Crystalline phase
PbO	Aldrich	99.9	0.8	n.a.	3.9	Orthor./tetrag.
ZrO <sub>2</sub>	Mel (SC 101)	99.7	23.0	0.04	0.9	Monoclinic
TiO <sub>2</sub>	Degussa (P 25)	99.0	48.4	0.03	0.2	Tetragonal
Nb <sub>2</sub> O <sub>5</sub>	Riedel–de Haen	99.9	1.2	1.01	11.0	Monoclinic
La <sub>2</sub> O <sub>3</sub>	Aldrich	99.99	n.a.	n.a.	n.a.	Hexagonal

<sup>a</sup> Referred to the powder crystallite size.

<sup>b</sup> Median diameter of powder agglomerates.

Table 2  
Properties of PLZTN powders.

S.S.A. [m <sup>2</sup> /g]	<i>d</i> <sub>50</sub> [μm]	pH <sup>a</sup>	ζ potential <sup>a</sup> [mV]
3.4	0.708	10.24	+41.8

<sup>a</sup> Referred to the powders dispersed in water.

agglomeration for the presence of ionizable groups [–COO(NH<sub>4</sub>)] that can dissociate in water [17] and a steric repulsion due to the hindrance of the macromolecule adsorbed on the surface powders. Suspensions were prepared by mixing the powders in deionized water, previously added with proper amounts of Duramax D-3021, and subjected to ball milling for 16 h in 100 cm<sup>3</sup> plastic jars with zirconia spheres as milling media. Subsequently, an acrylic latex binder emulsion at 55 wt% (Duramax B-1000, Rohm & Haas, Philadelphia, USA) was mixed with the slurry and the whole system was stirred for further 15 min. The binder provides easy handling of the green tapes after drying and in all operations before sintering. Finally, the surfactant – an aqueous emulsion at 75 wt% of tetramethyldecyldiol ethoxylated (Surfynol SE-F, Air Products Chemicals, Utrecht, The Netherlands) – was added to improve the wetting properties of the suspension on the carrier tape. The slurries obtained in this manner were gently stirred for further 90 min and immediately submitted to the rheological characterization and tape casting.

Table 3  
Formulations of aqueous PLZTN suspensions.

Suspension	Powder [vol%] <sup>a</sup>	Dispersant [wt%] <sup>b</sup>	Binder [vol%] <sup>c</sup>	Surfactant [mg/cm <sup>3</sup> ] <sup>d</sup>
A	42	0.80	70	5
B	44	0.80	70	5
C	40	0.80	70	5
D	42	0.80	60	5
E	42	0.80	50	5
F	42	0.40	70	5
G	42	0.32	50	5
H	42	0.80	70	10

<sup>a</sup> Percentage volume fraction of powder with respect to the volume of suspension after dispersant solution addition (neglecting the dispersant volume), and before any other additives addition.

<sup>b</sup> Percentage mass fraction of polyelectrolyte molecules of dispersant with respect to the mass of PLZTN powder.

<sup>c</sup> Percentage volume fraction of acrylic molecules of binder with respect to the volume of PLZTN powder.

<sup>d</sup> The concentration of surfactant is referred to the overall suspension volume.

In order to investigate the effect of organic additives on flow behavior, eight formulations differing for the content of only one component with respect to a reference suspension (indicated as A), were considered, except for one suspension (named G) that differs for the concentrations of two components (Table 3). The chosen set of suspensions can be considered as representative of the formulations of aqueous PLZTN suspensions for tape casting.

### 2.3. Rheological characterization

The flow behavior of PLZTN suspensions was characterized with a controlled-stress rotational rheometer (Bohlin C-VOR 120, Malvern, UK) equipped with parallel plate sensor with diameter 20 mm (PP20) and forcing the gap to 1 mm. In order to prevent evaporation, the free surface of the sample between the plates was covered with silicon oil. Measurements were carried out under continuous flow conditions applying a torque (shear stress) to the fluid and registering the corresponding angular velocity (shear rate) at steady state conditions. Flow curves were determined by increasing the shear stress by a step procedure in 24 steps from 0.351 to 162 Pa. In some cases the experimental points at the lower and higher shear stresses were not considered because not significant.

### 2.4. Tape casting

The tape casting was conducted, after degassing and filtration of the suspensions, on a silicon-coated polyethylene terephthalate carrier film (Mylar, Douglas-Hanson, Hammond, WI, USA) by means of the doctor blade technique using a single blade geometry casting head. All the castings were performed with the height of the blade set at 200 μm and a carrier speed of 65 cm/min. The tapes were allowed to dry for 12 h at room temperature without airflow, and then green tapes were cut, removed from the support and subjected to eye inspection. A tape was considered satisfactory if flawless (i.e., free from holes, voids and other defects), easily removable from support without release, and easily processed after removal.

## 3. Background

### 3.1. Viscous models

In this section we will briefly recall five rheological models that can be applied to describe the flow behavior of suspensions

employed in the tape casting process. All these models have been applied to the viscous responses of our set of suspensions to elucidate their suitability to represent those behaviors. The Bingham model [7]:

$$\sigma = \sigma_0 + \eta_\infty \dot{\gamma}, \quad (1)$$

contains two parameters, the yield stress  $\sigma_0$  and the plastic viscosity  $\eta_\infty$ . Flow conditions occur only for stress values exceeding the yield stress; a Newtonian plateau, quantified by  $\eta_\infty$ , is achieved at high-shear rates. The Herschel–Bulkley equation [10] can be considered a modified version of this classical plastic model, where the Newtonian viscous contribution is replaced by a power-law term:

$$\sigma = \sigma_0 + \kappa \dot{\gamma}^n, \quad (2)$$

where  $\kappa$  is referred as consistency and  $n$  is a parameter that determines the rate of the viscosity change with shear rate. Both the equations must be coupled with the yield condition that separate the liquid-like from solid-like behavior:  $\dot{\gamma} = 0, \sigma \leq \sigma_0$ . Accordingly, both the aforementioned models involve a distinction between *yielded* and *unyielded* regions within the material, in presence of wide stress distributions encompassing the yield condition. However, when more sophisticated rheometers are used for the rheological characterization, the existence of high-viscosity Newtonian plateau is often detected at low-shear stresses for materials normally classified as plastic. As consequence of these experimental evidences the “yield stress” should be considered as an engineering parameter and the plastic models as useful tools for describing the viscous behavior in the stress range exceeding the dramatic viscosity drop typical of apparently plastic fluids. In addition, the use of a rheological model described by two equations valid in different ranges of the shear stress applied, as well as of other rheological models based on the yield criterion, is troublesome if an algorithm, accounting for the plastic behavior, must be implemented for flow simulation in complex geometries. To solve this problem, Papanastasiou proposed a modified version of the Bingham equation suitable to describe the apparently plastic behavior with a single equation from low to high shear [8]:

$$\sigma = \sigma_0 [1 - \exp(-m\dot{\gamma})] + \eta_\infty \dot{\gamma}, \quad (3)$$

The yield stress contribution is graded by the parameter  $m$  through the exponential factor; for sufficiently high  $m$  values the stress–shear rate curve approaches the Binghamian behavior even at very low-shear rates, while low  $m$  values result into shear-thinning profiles. The product  $\sigma_0 m$  measures the difference between the two Newtonian plateaus attained at low- and high-shear conditions. Usually, more than three parameters are needed to describe the flow curves of shear-thinning fluids. One of the simplest models able to fit such a behavior is given by the Cross equation [7]:

$$\frac{\eta - \eta_\infty}{\eta_0 - \eta_\infty} = \frac{1}{1 + (\lambda \dot{\gamma})^n}, \quad (4)$$

where  $\lambda$  is a characteristic time whose inverse marks the onset of viscosity decrease,  $n$  is an exponent (whose value is comprised between 0 and 1) that determines the degree of shear-thinning, and  $\eta_0$  and  $\eta_\infty$  are the asymptotic viscosity values at zero and infinite shear rates, respectively. This model can be applied with satisfactory fitting quality only in the case of symmetric shape of the flow curve with respect to the inflection point of the curve itself, i.e., when the drop-off in viscosity from  $\eta_0$  is mirrored by an equivalent leveling-off towards  $\eta_\infty$ . More complex behaviors imply the use of a higher number of adjustable parameters. These problems related to the asymmetric shape of the flow curve appear more evident in the case of apparently plastic behavior when data are plotted in the  $\log \eta - \log \sigma$  diagram. In order to better describe the gradual fall-off in viscosity before the sharp drop and the (gradual or sharp) leveling-off towards  $\eta_\infty$ , a modification of Ellis equation was proposed by Roberts et al. [10], and it will be referred hereafter as RBC model. The Ellis equation is formally analogous to the Cross model, but the viscosity is expressed as a function of shear stress instead of shear rate. The RBC model fits more shapes of the flow curve, since the original parameters of the Ellis equation,  $\eta_0$  and  $\eta_\infty$ , are replaced by two functions of shear stress:  $\eta'_0(\sigma)$  and  $\eta'_\infty(\sigma)$ , respectively. Therefore the set of equations describing the RBC model is the following:

$$\frac{\eta - \eta'_\infty}{\eta'_0 - \eta'_\infty} = \frac{1}{1 + (\sigma/\sigma_c)^m}, \quad (5)$$

$$\eta'_0 = \frac{\eta_0}{1 + (\sigma/\sigma_1)^p}, \quad (6)$$

$$\eta'_\infty = \eta_\infty [1 + (\sigma/\sigma_2)^s], \quad (7)$$

The exponents  $m$  and  $p$  are positive real numbers, while  $s$  is negative. Eqs. (6) and (7) allow a better description of the transition from the low-shear Newtonian plateau to the viscosity fall-off region, and then to the following leveling-off at higher shear stresses, respectively. The parameters  $\sigma_c$ ,  $\sigma_1$ , and  $\sigma_2$  are critical stresses and their relative order is  $\sigma_1 < \sigma_c < \sigma_2$ . The lowest one locates the end of the low-shear stress Newtonian plateau and the beginning of the gradual fall-off in viscosity,  $\sigma_c$  individuates the beginning of the sharp viscosity drop, and  $\sigma_2$  marks the starting point of the transition to the high-shear stress Newtonian plateau.

In Section 4.2 it will be shown how these models fit the experimental viscosity data obtained for the set of suspensions considered. Moreover, the performances and suitability of each equation with reference to the tape casting process will be discussed.

### 3.2. Flow simulations

In the tape casting process, modeling and simulation are used mostly for the description of the fluid flow under the blade and the calculation of the tape thickness; in both cases, experimental data about fluid (viscosity, density) and processing parameters (carrier velocity, blade height, length and width of channel) are required. The flow under the blade is generally



represented as a combination of two flow patterns: the parabolic profile of the velocity due to the hydrostatic pressure of the fluid in the reservoir, and the linear velocity profile of the plane Couette flow due to the drag of the carrier tape (or to the motion of the casting head). These two flows are additive only for Newtonian suspensions, which is a behavior that hardly is encountered with aqueous ceramic slurries for tape casting. For non-Newtonian fluids the solution is obtained by coupling the rheological model with the continuity and momentum equations, and taking into account the boundary conditions on pressure gradient and moving substrate [4]. Chou et al. [11] calculated tape thickness obtained with a Newtonian slurry from the aforementioned parameters. The subsequent efforts were always directed towards the flow simulation of non-Newtonian suspensions, for which plastic or generalized Newtonian expressions for viscosity were used. In those cases, the fitting of rheological data with appropriate models is necessary, as the viscosity changes with shear rate in the range involved in tape casting process. Loest et al. [12] proposed a simulation procedure to numerically retrieve the shape of the free surface of suspension after the blade; their calculations proved to be consistent with measurements performed with the shadow projection method. In another work [13], Loest et al. applied the Papanastasiou model to a FEM simulation of the flow pattern in the reservoir and in the flow channel for the tape casting of an organic-based alumina slurry. According to the model, the yield stress is made similar to a “critical” stress which marks the transition from the lower Newtonian plateau to marked flow conditions in pseudoplastic models, but the distinction between yielded and unyielded regions is nevertheless present. Simulations indicated that tapered reservoirs avoid the formation of vortices and limit the wideness of unyielded areas (i.e., high-viscosity areas corresponding to low-shear stress). Pitchumani and Karbhari [4] developed a fluid flow model for tape casting in which an Ostwald–de Waele power-law relationship is used to describe the viscous behavior of generalized Newtonian fluids. They calculated the tape thickness of a perovskite ceramic slurry for different carrier speeds in dependence of geometric parameters such as the height of the slurry in the reservoir, the height and length of the channel under the blade, and power-law model parameters depending on characteristics of the fluid. The same equation has been successively applied to an organic alumina slurry by Tok et al. [14], and their calculations proved to be closer to experimental results, in comparison to the simple linear

superposition of hydrostatic and drag contributions to flow. Other authors [15,16] considered Bingham plastic flow models for determining the tape thickness; in fact the yield stress approximation at low shears is consistent if it is taken into account that the tape thickness is controlled by the mass flow under the blade that is a relatively high-shear stress process. The approach of Joshi et al. [16] appears particularly attractive, as they consider the velocity profile in the channel under the blades as part of a fully developed profile in an imaginary channel. This model has been compared with the results in literature and proved to be really effective.

## 4. Results and discussion

### 4.1. Influence of formulation on the flow properties

The effects produced by composition changes on the flow behavior of the systems can be more easily evidenced by comparing the parameters of the viscous models. As it will be evident from Section 4.2, the RBC model provides the best-fitting for the aqueous PLZTN suspensions considered, and then its parameters will be used in the following analysis of the effects of powder and organic additives contents. The fitting procedure, based on non-linear least-squares method, was performed starting from reasonable guess values chosen on the basis of experimental data. The exponents  $m$  and  $p$  were imposed to be positive,  $s$  negative, and the following order were forced  $\sigma_1 < \sigma_c < \sigma_2$ . By using such constraints the parameters shown in Table 4 were obtained, where the end values of the objective function (O.F.), defined as in the following, are indicated as well:

$$\text{O.F.} = \sum_{i=1}^N \left( 1 - \frac{\eta_{i,\text{calc}}}{\eta_{i,\text{exp}}} \right), \quad (8)$$

where  $N$  is the number of fitted experimental points, and  $\eta_{i,\text{calc}}$  and  $\eta_{i,\text{exp}}$  are the viscosity calculated with the RBC model and experimentally measured, respectively.

The main parameters characterizing the flow behavior are the viscosities  $\eta_0$  and  $\eta_\infty$ , which correspond to the Newtonian behavior at low- and high-shear conditions, respectively, the critical stress  $\sigma_c$ , that marks the onset of the sharp viscosity drop from the upper Newtonian plateau and the exponent  $m$ , that gives the degree of (apparent) plasticity (the higher is  $m$ , the quicker is the viscosity drop). The  $\eta_0$ ,  $\sigma_c$ , and  $m$  values are

Table 4  
RBC model parameters.

Suspension	$\eta_0$ [ $\times 10^3$ Pa s]	$\eta_\infty$ [Pa s]	$\sigma_1$ [Pa]	$\sigma_c$ [Pa]	$\sigma_2$ [Pa]	$m$ [–]	$p$ [–]	$s$ [–]	O.F.
A	33.7	0.10	0.53	3.25	19.0	9.91	1.83	–2.84	0.2818
B	79.4	0.17	1.12	4.45	35.3	9.26	1.37	–2.57	0.1397
C	17.4	0.08	1.03	1.95	16.2	6.12	2.46	–2.33	0.0632
D	34.4	0.11	1.71	5.01	40.1	7.31	2.24	–2.62	0.2215
E	52.4	0.13	3.18	4.49	36.1	9.51	1.65	–2.69	0.1221
F	18.9	0.17	0.99	2.61	33.9	6.58	2.94	–1.37	0.0852
G	29.0	0.14	0.49	2.16	8.68	14.3	1.60	–2.35	0.1061
H	45.0	0.12	2.67	3.64	28.3	8.85	3.16	–2.60	0.0864

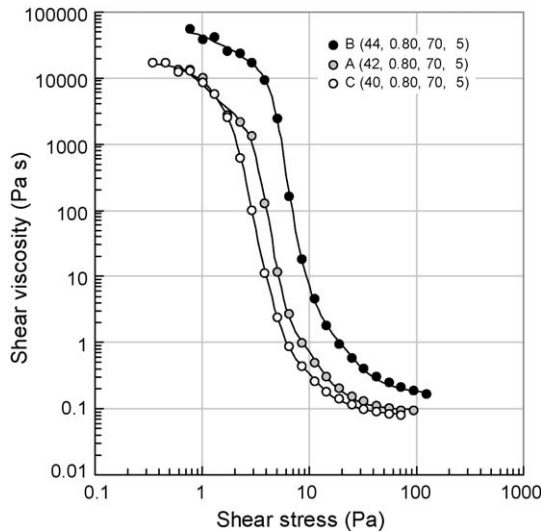


Fig. 1. Solids loading effect on the flow curves of PLZTN suspensions. The solid lines represent the fitting with the RBC model.

affected by the state of agglomeration of suspensions, while the high-shear viscosity  $\eta_\infty$  is determined mostly by the solids content. At high-shear stresses, in fact, the particle aggregates are broken down by the high viscous forces that dominate on interparticle forces and Brownian motion. The higher is the solids content, the higher is the high-shear viscosity  $\eta_\infty$ , but it does not provide significant information on the agglomeration of the systems and therefore on the additive effects. Therefore the following comparison will be mainly focused on the other three parameters. In this case we refer to the flow curves of Figs. 1–4, and to the corresponding values parameters summarized in Table 4.

#### 4.1.1. Solids loading effect

The effect of solids loading can be deduced by comparing the reference slurry A with suspensions B and C, prepared with higher and lower powder contents, respectively. As solids

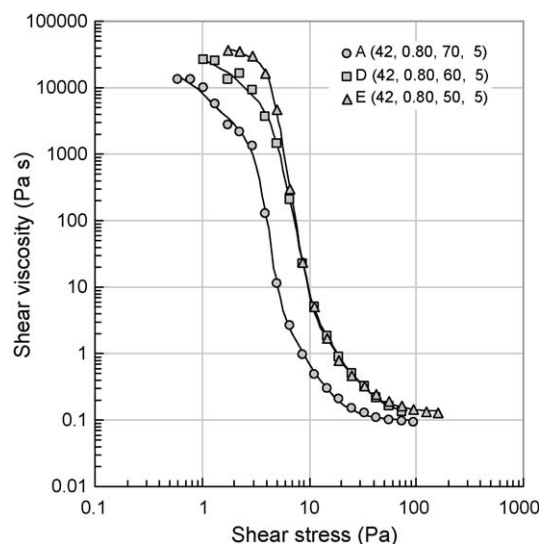


Fig. 2. Binder content effect on the flow curves of PLZTN suspensions. The solid lines represent the fitting with the RBC model.

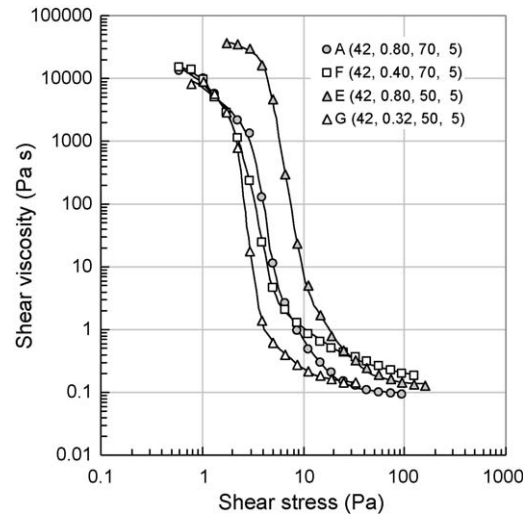


Fig. 3. Dispersant content effect on the flow curves of PLZTN suspensions. The solid lines represent the fitting with the RBC model.

loading increases,  $\eta_0$ ,  $\eta_\infty$ ,  $\sigma_c$ , and  $m$  increase, more evidently above 42 vol% (passing from 42 to 44 vol%  $m$  is substantially constant). The flow curves are shifted vertically (Fig. 1). In particular, the increase of low-shear viscosity  $\eta_0$  and critical stress  $\sigma_c$  are the results of the increased aggregation state of the dispersed phase, which makes more difficult to break up the particle aggregates and to produce an appreciable flow. In such conditions the effective volume fraction of the dispersed phase is higher than the nominal one and a small increase in solids loading above 42 vol% (from A to B) results into a closer approach to the maximum packing condition, and, consequently, into a steeper increase of  $\eta_0$ , as described by Krieger–Dougherty or Quemada equations [7].

#### 4.1.2. Binder effect

The influence of binder content can be analyzed through the comparison of the flow behavior of suspensions A, D, and E

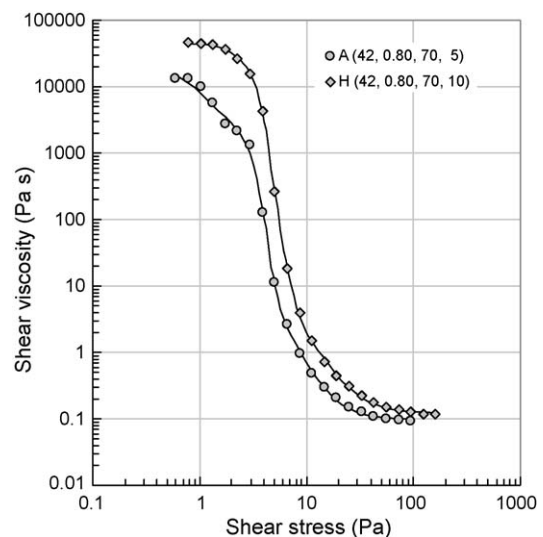


Fig. 4. Surfactant content effect on the flow curves of PLZTN suspensions. The solid lines represent the fitting with the RBC model.

(Fig. 2). The binder is added in relevant amount as concentrated aqueous emulsion (55 wt%). This leads to a dilution of the resulting ceramic dispersions in terms of powder volume fraction. Thus, the decrease of the binder content from 70 vol% (corresponding to the reference suspension A) to 60 vol% (suspension D), down to 50 vol% (suspension E), is accompanied by an increase in the powder volume fraction that changes from 26.5 vol% (A) to 27.9 vol% (D), up to 29.5 vol% (E). The higher solids loading increases  $\eta_0$  and  $\eta_\infty$  and also  $\sigma_c$  and  $m$  even if for these two latter the scattering of the data at low-shear results not very accurate values. The increase of viscosity with the decrease of the binder content might appear in disagreement with the idea that the introduction of binder amount increases the suspension viscosity due to the particles agglomeration through a binder-promoted bridging mechanism between solid particles (*bridging flocculation*). However, the dilution effect due to the high water content in binder emulsion is predominating on the expected effect of bridging flocculation due merely to the binder molecules. So, the overall dilution effect screens the real role played by the binder molecules that cannot be evinced from the flow curves.

#### 4.1.3. Dispersant effect

An optimal dispersant amount let to obtain a well-dispersed suspension with low viscosity. Below that value the system is not sufficiently stabilized, while exceeding it the dispersant is not adsorbed on the surfaces of the particles, thus remaining free in the continuous liquid phase. If the not-adsorbed polymer concentration overcomes a critical value, a flocculation mechanism related to osmotic effects (*depletion flocculation*) can occur (especially in highly concentrated suspensions) promoting the increased degree of agglomeration and viscosity. By comparing the flow curves of suspensions A and F (Fig. 3), we can observe that the decrease of dispersant content (the one of F is the half of A: 0.40 wt% instead of 0.80 wt%), corresponds to a decrease of  $\eta_0$ ,  $\sigma_c$ , and  $m$  (while  $\eta_\infty$  increases). This suggests that 0.80 wt% is an excessive amount of dispersant affecting the suspension stability by depletion flocculation mechanism. This is confirmed, and still more evident, if more concentrated suspensions are prepared. In fact, in such systems, when the interparticle distance decreases, the probability of flocculation due to the displacement of polymer chains from the space between two approaching particles increases; this results in a more complex structure, characterized by higher viscosity values with respect to more diluted systems. This is evident if the suspensions E and G are compared (Fig. 3); they differ also in dispersant content (0.80 and 0.32 wt%, respectively), but possess higher solids loading compared to suspensions A and F (due to the lower binder content). The solid volume fraction for A and F is about 26.5 vol%, while the one for E and G is about 29.6 vol%. They show rather different values of  $\eta_0$  and  $\sigma_c$ , confirming the hypothesis of depletion flocculation due to excessive dispersant concentration. The strong increase of  $m$  could be a signal that a concentration of 0.32 wt% is too low amount of dispersant. The high-shear viscosities are similar, as expected. From the flow curves it can be noted that the suspensions with the higher

content of dispersants (A and E) approach the higher Newtonian plateau more gradually than the suspensions with lower contents of dispersants (F and G).

#### 4.1.4. Surfactant effect

The surfactant content influences the flow properties, too (Fig. 4). In the suspensions A and H (having contents of surfactants of 5 and 10 mg/cm<sup>3</sup>, respectively) a comparison between  $\eta_0$  and  $\sigma_c$  values shows that H has a higher viscosity and structuring degree than A, so that a surfactant-driven destabilization of the system occurs. This higher flocculation for suspension H is probably due to a competitive adsorption process between dispersant and surfactant on charged particle surfaces. The lower efficiency of surfactant to screen the particles, compared to the macromolecules of polyelectrolyte, leads to a worsened system stability.

#### 4.1.5. Tape casting performance evaluation

The comparison of the parameters obtained by fitting the experimental data with an appropriate model, to analyze the concentration effect of the components on the flow properties, represents a valuable tool for an *a priori* selection of proper formulations for the tape-cast suspensions. However, the optimization of the flow properties represents only an aspect of the problem because the choice of the formulation is strongly related also with the resulting casting performances. Therefore, this approach requires also that preliminary casting performances with a representative set of formulations were previously evaluated. Given this necessary check was done this route could avoid expensive and time-consuming casting experiments, allowing at the same time to foresee the variation of flow behavior induced by changes in the formulation.

The quality of the tapes obtained, shown in Fig. 5 and summarized in Table 5 for four significant formulations, well evidences how other issues must be taken into account to improve the whole tape casting process. In fact, all the suspensions considered were pourable, but some of them were affected by adhesion problems. A good wettability and a tape free from flaws was obtained by doubling the content of surfactant (suspension H), even if the presence of the surfactant increases the viscosity suspension, thus making more difficult the casting. Therefore, good enough flow properties of the suspensions is the main critical issue to have good tapes, but other aspects like, e.g., the wettability of the carrier, must be considered as well. This makes more difficult the task because any additive added, even if not related with the improvement of the flow properties, could affect the rheology of the system thus compromising the flowability. In this view performing a

Table 5  
Performances of the cast tapes.

Suspension	Thickness ( $\mu\text{m}$ )	Wettability	Defects	Tape
A	n.d.	n.d.	n.d.	Not obtained
D	100	Low	Few	Partially obtained
B	130	Low	Few	Partially obtained
H	110	High	None	Obtained

screening of the effect of those additives (nature/amount) on the flow properties is an important, necessary step to optimize the whole process.

#### 4.2. Applicability of viscous models for flow simulation in tape casting process

In order to reproduce the flow patterns in tape casting process by using numerical simulations via finite element method (FEM) or other packages, the knowledge of a rheological model for the suspensions is necessary. Through flow simulations it is possible: (1) to find out the tape thickness starting from operating parameters and properties of the complex fluid, and (2) to evaluate the velocity profiles either in the channel or in the reservoir (as described in Section 3.2). For these purposes the use of the RBC model appears redundant. In fact, the tape casting process involves relatively high-shear stresses and the flow behavior of suspensions in such regions is fairly well represented by plastic or pseudoplastic models, that are characterized by a lower number of parameters than the RBC model. Therefore, for flow simulations it is convenient to use models that allow easier calculation. The same considerations can be applied to the simulation of flow patterns in the low-shear stress area of reservoir. In fact, it is possible to provide a good fitting of the experimental data in this range by using pseudoplastic or plastic models, involving a lower number of parameters.

Models that are preferably used for calculations are the plastic-type Bingham and Herschel–Bulkley models (Eqs. (1) and (2), respectively) for the high-shear range, and the plastic Papanas-

tasiou model or the pseudoplastic Cross model (Eqs. (3) and (4), respectively) for the low-shear range. As the flow curves for the eight aqueous PLZTN suspensions here considered have roughly the same qualitative shape (as evident from Figs. 1–4), the analysis is reported only for suspension B, which has been chosen as reference. It has been verified that the same considerations are applicable also to the other suspensions of the set.

Since the investigated experimental window ranges from low- to high-shear stresses, flow curves including the two Newtonian plateaus have been obtained. This flow behavior is well represented not only by RBC model, but also by Cross and Papanastasiou models (Fig. 6a and b). The Cross model appears to be really effective and its performance is close to that of RBC model, while the Papanastasiou model fits the experimental data with less precision, though allowing easier calculation (3 parameters instead of 4). Thus, this latter model could be an interesting compromise between fitting performance and ease of calculation, if high accuracy is not required for the technological problem considered. It is stated that these two models are appropriate, with different degree of approximation, to describe the flow behavior for any shear stress value. Nevertheless, for high-shear stress range simpler models can be used to represent the data, and Cross and Papanastasiou models should be limited to the low-shear modeling.

The high-shear flow of suspension under the blade is now considered. The shear rate involved in this process can be approximately determined by the ratio of carrier speed and height of flow channel [5]. By taking into account typical values for these two operating parameters, the range of possible shear

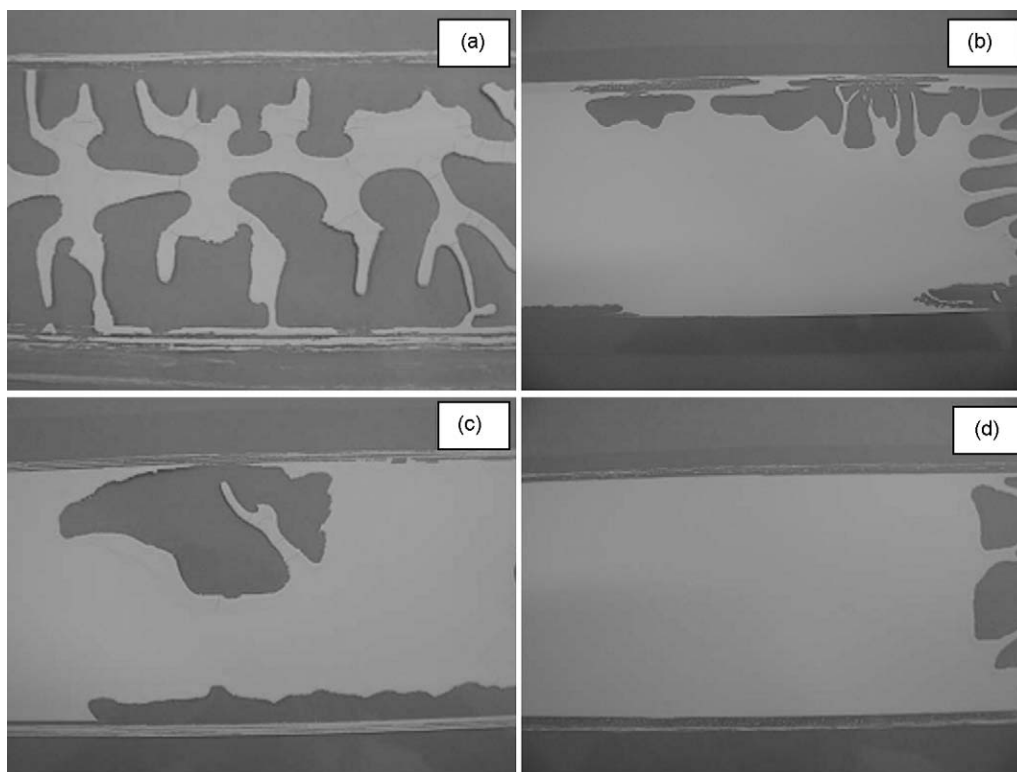


Fig. 5. Tape performance analysis: (a) suspension A (42/0.80/70/5), (b) suspension D (42/0.80/60/5), (c) suspension B (44/0.80/70/5), and (d) suspension H (42/0.80/70/10).



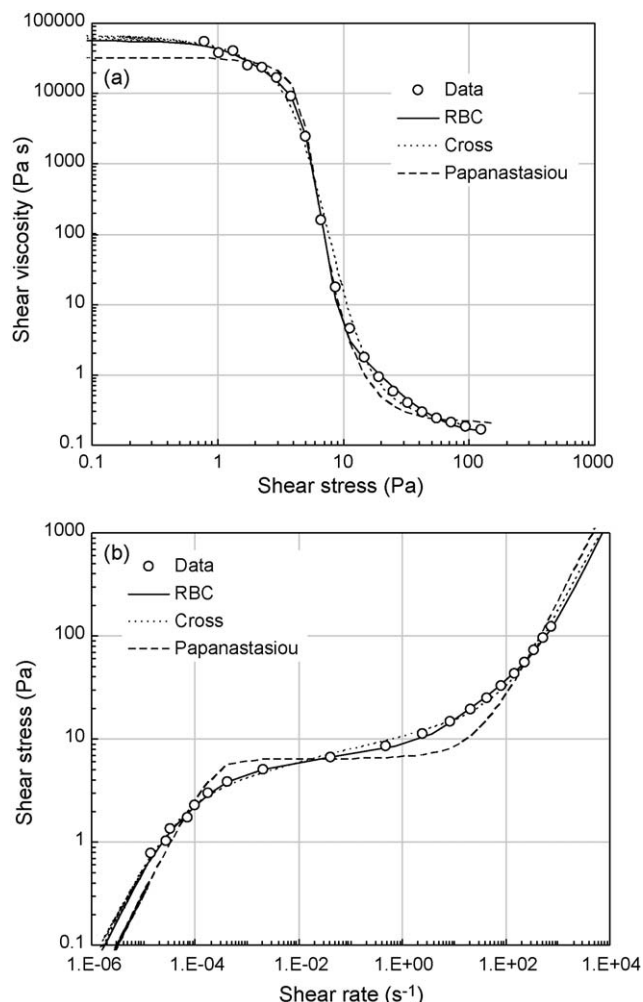


Fig. 6. (a) Flow curve of suspension B in terms of viscosity vs. shear stress. Comparison between Cross, Papanastasiou and RBC models. (b) Flow curve of suspension B in terms of shear stress vs. shear rate. Comparison between Cross, Papanastasiou and RBC models.

rates involved in the process is  $2.5\text{--}750\text{ s}^{-1}$ . In order to calculate the tape thickness, operating parameters and fluid characteristics (density and viscosity) are required. If the viscosity dependence on shear rate in the previous defined range is expressed by a rheological model, its value can be determined for every shear rate in the range.

In Fig. 7a and b the performances of Bingham and Herschel–Bulkley plastic models, compared to RBC equations, are shown for the suspension B. The fitting was performed by restricting the experimental window to the high-shear values (grey areas in previous figures), which correspond to the shear range involved in the flow of the suspensions under the blade ( $2.5\text{--}750\text{ s}^{-1}$  for shear rate and  $15\text{--}150\text{ Pa}$  for shear stress, roughly). It is interesting to note how the evidenced narrow range of shear rates corresponds to the working range of the common rate-controlled rheometers. As shown, the RBC model is still the best-fitting model, but its use for such a restricted area appears redundant. In fact, the two plastic models allow to obtain a satisfactory fit of the experimental data with a lower number of parameters, thus enabling an easier calculation. Data are fairly well represented by Herschel–Bulkley model, while the

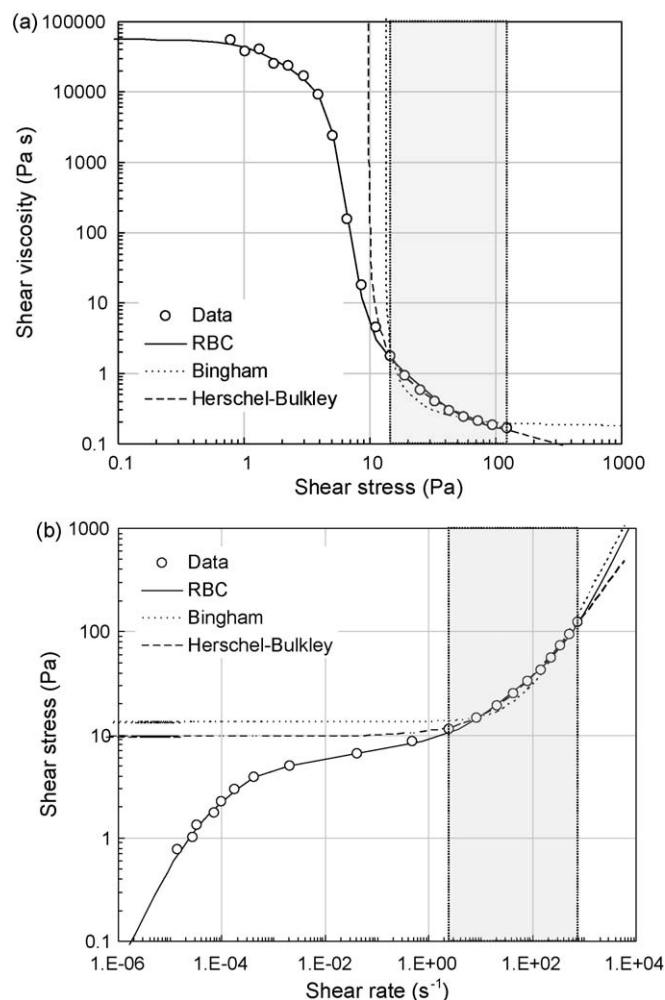


Fig. 7. (a) Flow curve of suspension B in terms of viscosity vs. shear stress. Comparison between plastic models at high-shear stresses. (b) Flow curve of suspension B in terms of shear stress vs. shear rate. Comparison between plastic models at high-shear rates.

Bingham equation appears less precise. The results obtained with these two plastic models, for the whole set of suspensions considered, are listed in Table 6. The parameter variation with respect to the components content reflects the same trend of RBC parameters, as already discussed in the previous section. This enforces the considerations on the effect of components on flow properties as well. A comparison between systems based on the parameter analysis could be carried out employing any

Table 6  
Parameters of plastic models (Bingham and Herschel–Bulkley).

Suspension	Bingham		Herschel–Bulkley		
	$\sigma_0$ [Pa]	$\eta_\infty$ [Pa s]	$\sigma_0$ [Pa]	$\kappa$ [Pa s <sup>n</sup> ]	$n$ [–]
A	6.5	0.10	5.2	0.6	0.71
B	13.3	0.17	9.6	1.1	0.70
C	5.0	0.08	3.3	0.7	0.65
D	5.9	0.17	4.2	4.9	0.39
E	11.4	0.14	8.8	1.1	0.68
F	5.0	0.28	3.6	1.3	0.68
G	2.4	0.15	2.9	0.4	0.79
H	8.7	0.13	4.7	1.5	0.61

model, but when the widest experimental window must be considered, Papanastasiou, Cross or RBC models should be applied. Experimental data in this wide shear rate range are obtainable with stress-controlled rheometers.

## 5. Conclusions

In this paper the performances of some rheological models applied to aqueous PLZTN suspensions for tape casting were investigated. In particular, two plastic models (Bingham and Herschel–Bulkley), a modified plastic model (Papanastasiou), and two pseudoplastic models (Cross and RBC) were considered. We applied the aforementioned models to experimental data obtained for a suitable set of PLZTN tape casting formulations to see the effect of additives on the flow properties. This approach enabled us to obtain useful information about the optimization of the formulations in the set up of the tape casting process, even if such information must be coupled with the ones obtained by the evaluation of the tape casting performances. The analysis of the models also permitted us to determine the most effective model in representing the rheological behavior of the considered suspensions and to identify the proper application range for each model. It has been verified that RBC model, due to its high number of parameters, is the best-fitting model for the set of suspensions examined and it was used for the parameter-based comparison between systems. Concerning the implementation of the models for computer flow simulations, in order to solve technological problems affecting the tape casting process, Cross model is suggested for low-shear modeling. Herschel–Bulkley model is more appropriate for the high-shear range, that corresponds to the flow under the doctor blade, and can be investigated with the common rate-controlled rheometers. Papanastasiou and Bingham equations allow a less precise fit with respect to the formerly cited ones, while RBC model with its eight parameters appears redundant for that purpose.

## Acknowledgment

The authors would like to thank Claudio Capianni (CNR-ISTEC, Faenza) for the synthesis of PLZTN powders. Financial

support by CNR under the Free Theme Research “Study of Rheological and Colloidal Properties of Disperse Ceramic Systems for the Optimization of Products and Processes”, Grant 405 is gratefully acknowledged.

## References

- [1] D. Hotza, P. Greil, Review: aqueous tape casting of ceramic powders, *Mater. Sci. Eng. A* 202 (1995) 206–217.
- [2] R.E. Mistler, Tape casting the basic process for meeting the needs of the electronics industry, *Am. Ceram. Soc. Bull.* 69 (1990) 1022–1026.
- [3] A. Kristoffersson, E. Roncari, C. Galassi, Comparison of different binders for water-based tape casting of alumina, *J. Eur. Ceram. Soc.* 18 (1998) 2123–2131.
- [4] R. Pitchumani, V.M. Karbhari, Generalized fluid flow model for ceramic tape casting, *J. Am. Ceram. Soc.* 78 (1995) 2497–2503.
- [5] B. Bitterlich, C. Lutz, A. Roosen, Rheological characterization of water-based slurries for the tape casting process, *Ceram. Int.* 28 (2002) 675–683.
- [6] H.A. Barnes, The yield stress – a review or “παντα ρει” – everything flows? *J. Non-Newtonian Fluid Mech.* 81 (1999) 133–178.
- [7] H.A. Barnes, J.F. Hutton, K. Walters, *An Introduction to Rheology*, Elsevier, Amsterdam, 1989.
- [8] T.C. Papanastasiou, Flows of materials with yield, *J. Rheol.* 31 (1987) 385–404.
- [9] P.R. Souza Mendes, E.S.S. Dutra, Viscosity function for yield-stress liquids, *Appl. Rheol.* 14 (2004) 296–302.
- [10] G.P. Roberts, H.A. Barnes, P. Carew, Modelling the flow behavior of very shear-thinning liquids, *Chem. Eng. Sci.* 56 (2001) 5617–5623.
- [11] Y.T. Chou, Y.T. Ko, M.F. Yan, Fluid flow model for ceramic tape casting, *J. Am. Ceram. Soc.* 70 (1987) C280–C282.
- [12] H. Loest, E. Mitsoulis, S. Spauszus, Free surface measurement and numerical simulations of ceramic tape casting, *Interceram* 42 (1993) 80–84.
- [13] H. Loest, R. Lipp, E. Mitsoulis, Numerical flow simulation of viscoplastic slurries and design criteria for a tape casting unit, *J. Am. Ceram. Soc.* 77 (1994) 254–262.
- [14] A.I.Y. Tok, F.Y.C. Boey, Y.C. Lam, Non-Newtonian flow model for ceramic tape casting, *Mater. Sci. Eng. A* 280 (2000) 282–288.
- [15] G. Zhang, Y. Wang, J. Ma, Bingham plastic fluid flow model for ceramic tape casting, *Mater. Sci. Eng. A* 337 (2002) 274–280.
- [16] S.C. Joshi, Y.C. Lam, F.Y.C. Boey, A.I.Y. Tok, Power law fluids and Bingham plastics flow models for ceramic tape casting, *J. Mater. Proc. Technol.* 120 (2002) 215–225.
- [17] J.H. Feng, F. Dogan, Aqueous processing and mechanical properties of PLZT green tapes, *Mater. Sci. Eng. A* 283 (2000) 56–64.
- [18] C. Pagnoux, T. Chartier, M. de, F. Granja, F. Doreau, J.M. Ferreira, J.F. Baumard, Aqueous suspensions for tape-casting based on acrylic binders, *J. Eur. Ceram. Soc.* 18 (1998) 241–247.